Synthesis and characterization of an O^6-2′-deoxyguanosine-alkyl-O^6-2′-deoxyguanosine interstrand cross-link in a 5′-GNC motif and repair by human O^6-alkylguanine-DNA alkyltransferase†

Francis P. McManus,[a] Qingming Fang,[b] Jason D. M. Booth,[a] Anne M. Noronha,[a] Anthony E. Pegg[b] and Christopher J. Wilds*[a]

Received 7th May 2010, Accepted 28th June 2010
DOI: 10.1039/c0ob00093k

O^6-2′-Deoxyguanosine-alkyl-O^6-2′-deoxyguanosine interstrand DNA cross-links (ICLs) with a four and seven methylene linkage in a 5′-GNC- motif have been synthesized and their repair by human O6-alkylguanine-DNA alkyltransferase (hAGT) investigated. Duplexes containing 11 base-pairs with the ICLs in the center were assembled by automated DNA solid-phase synthesis using a cross-linked 2′-deoxyguanosine dimer phosphoramidite, prepared *via* a seven step synthesis which employed the Mitsunobu reaction to introduce the alkyl lesion at the O^6 atom of guanine. Introduction of the four and seven carbon ICLs resulted in no change in duplex stability based on UV thermal denaturation experiments compared to a non-cross-linked control. Circular dichroism spectra of these ICL duplexes exhibited features of a B-form duplex, similar to the control, suggesting that these lesions induce little overall change in structure. The efficiency of repair by hAGT was examined and it was shown that hAGT repairs both ICL containing duplexes, with the heptyl ICL repaired more efficiently relative to the butyl cross-link. These results were reproducible with various hAGT mutants including one that contains a novel V148L mutation. The ICL duplexes displayed similar binding affinities to a C145S hAGT mutant compared to the unmodified duplex with the seven carbon containing ICLs displaying slightly higher binding. Experiments with CHO cells to investigate the sensitivity of these cells to busulfan and hepsulfam demonstrate that hAGT reduces the cytotoxicity of hepsulfam suggesting that the O^6-2′-deoxyguanosine-alkyl-O^6-2′-deoxyguanosine interstrand DNA cross-link may account for at least part of the cytotoxicity of this agent.

Introduction

Interstrand cross-links (ICLs) that are formed in DNA as a consequence of the action of bifunctional alkylating agents represent some of the most toxic lesions encountered by cells due to the obstruction of unwinding of the two strands, critical to the processes of DNA replication, transcription and recombination.[1] Interference with these key cellular processes by the presence of ICLs is the basis of the mechanism of action of bifunctional alkylating agents, such as mechlorethamine, that are used as cancer therapeutics.[2] However, the potency of these agents is reduced by the ability of cancer cells to repair the lesions resulting in an overall resistance to therapy.

In eukaryotic cells the repair of ICLs is a complex process with numerous repair pathways including nucleotide excision repair, homologous recombination and non-homologous end joining implicated in the removal of the damage.[3] Understanding the molecular basis of how ICL repair occurs will play an important role towards the development of new chemotherapeutic agents that may evade this process, thus increasing the efficacy of these drugs.

One approach employed in elucidating the roles various DNA repair pathways contribute in removing DNA ICLs involves the use of chemically synthesized oligonucleotides that contain representative lesions formed by bifunctional alkylating chemotherapeutics.[4,5,6] These oligonucleotides are designed to contain lesions linking specific atoms in DNA in well defined orientations and can be incorporated into plasmids for DNA repair experiments. This approach uses solid-phase synthesis which generates sufficient amounts of ICL DNA to enable structural studies and repair assays.[7,8,9,10,11]

Some of these ICLs are challenging to prepare synthetically. For example, the bifunctional alkylating agent hepsulfam (1,7-heptanediol disulfamate) which has been investigated clinically,[12] has been shown to form a cross-link between the N^7 atoms of guanines in 5′-GNC sequences (Fig. 1) as demonstrated through the use of mass spectrometry and identification of 1,7-bis(guanyl)heptane.[13] N^7-alkylated guanines are chemically unstable, for example the presence of N^7-methylguanine can result in an apurinic site in DNA or undergo ring opening to yield the ring opened formamido pyrimidine (Fapy) derivative.[14,15]

[a]*Department of Chemistry and Biochemistry, Concordia University, 7141 Sherbrooke St. West, Montréal, QC, Canada, H4B 1R6. E-mail: cwilds@alcor.concordia.ca; Fax: 514-848-2868; Tel: 514-848-2424 ext. 5798*
[b]*Departments of Cellular and Molecular Physiology and Pharmacology, The Pennsylvania State University College of Medicine, PO Box 850, Hershey, PA, USA, 17033*

† Electronic supplementary information (ESI) available: ^{1}H NMR and ^{31}P NMR of compounds **6a**, **6b**, **7a** and **7b**, HPLC chromatographs and MS spectra for oligonucleotide characterization and repair and binding data of hAGT to the ICL. See DOI: 10.1039/c0ob00093k

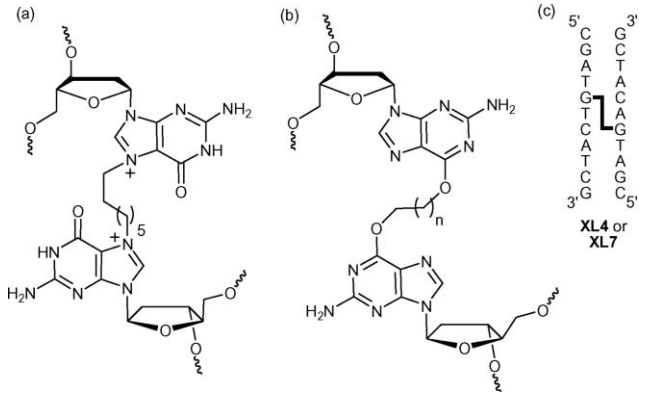

Fig. 1 Structures of the (a) N^7-2′-deoxyguanosine-heptyl-N^7-2′-deoxyguanosine cross-link induced by hepsulfam, (b) the O^6-2′-deoxyguanosine-alkyl-O^6-2′-deoxyguanosine cross-link (where $n = 3$ or 6) and oligomers (c) **XL4** and **XL7**.

In order to prepare oligonucleotides containing a cross-link that models the orientation of the lesion formed by hepsulfam, our group has explored methodologies to prepare ICL DNA that links the O^6 atoms of 2′-deoxyguanosine.[16] The O^6 atom of guanine is a known site of alkylation by chemotherapeutic drugs such as the methylating agent temozolomide and the chloroethylating agent carmustine which proceeds to form a guanine-cytosine ICL.[17]

Different chemical groups at the O^6 position of guanine have been incorporated by organic synthesis for numerous purposes including protection during oligonucleotide synthesis and as substrates for DNA repair studies.[18,19] Examples of synthetic methods that have been employed to introduce these groups include the post-synthetic modification of oligonucleotides containing the 2′-deoxyribonucleoside of 2-amino-6-methylsulfonylpurine and the Mitsunobu reaction.[19,20]

Using a combination of solution and solid-phase synthesis, a 5′-GNC ICL has been prepared (Fig. 1) which required a O^6-2′-deoxyguanosine-alkyl-O^6-2′-deoxyguanosine phosphoramidite that contains various protecting groups to permit orthogonal removal, enabling a unit of asymmetry to be engineered in the final ICL DNA duplex to allow for a clinically relevant staggered 1,3 orientation. The synthetic scheme to produce this amidite involved the Mitsunobu reaction which was selected due to its mild conditions, compatibility with all protecting groups employed and direct route to introduce alkyl linkers of various lengths. This method allows for the production of ICL duplexes to explore the influence of linker length in substrates of defined structure and for the systematic investigation of susceptibility to DNA repair mechanisms.

The ability of wild-type human O^6-alkylguanine-DNA alkyltransferase (hAGT) and some mutants to repair these ICLs was also investigated. O^6-Alkylguanine-DNA alkyltransferases (AGT) are a class of repair proteins that are found in numerous organisms whose role is to repair alkylation at the O^6 position of the guanine base and thus they play an important role in maintaining genomic integrity.[21] Alkylation at the O^6 position of guanine can be mutagenic, disrupting normal Watson–Crick base pairing leading to point mutations which may be fatal. The mechanism by which hAGT repairs alkylated DNA involves flipping the alkylated base out of the duplex and into the active site of the protein where transfer of the alkyl group from the O^6 position of guanine to a C145 residue occurs.[22] The protein can only act once due to the irreversible alkylation of C145, whereupon the protein is degraded by the ubiquitin pathway.[23] hAGT has been shown not only to repair small adducts at the O^6 position of guanine such as a methyl group but also larger groups such as benzyl and 4-(3-pyridyl)-4-oxobutyl.[24] The study of these novel ICL substrates to undergo repair by hAGT will contribute to the range of DNA substrates that can undergo repair *via* this pathway.

Results and discussion

Syntheses and characterization of the ICL duplexes

Interstrand cross-linked DNA repair studies require access to substrates of well defined structure. The bifunctional alkylating agent hepsulfam has been shown to alkylate specifically at the N^7 atom of 2′-deoxyguanosine in sequences containing a 5′-GNC motif placing a heptyl linkage between the two guanines.[13] Because they are synthetically challenging to prepare, we have focused on the synthesis of a cross-link that joins the O^6 atoms in this particular sequence motif. It should be emphasized that this specific cross-link has not been identified as a product of alkylation by hepsulfam. The methodology to produce this ICL was used to prepare duplexes containing alkyl linkages of various lengths to investigate the affect of linker length on ICL stability, structure and repair by hAGT. The chemotherapeutic agent busulfan (1,4-butanediol dimethanesulfonate) is another example of a bifunctional alkylating agent that has been used for the treatment of chronic myelogenous leukemia.[25] This agent introduces a butyl linkage between the nucleobases with the demonstration that this agent reacts with guanosine to form 1,4-di(7-guanosinyl)butane.[26] Mass spectrometry of the reaction products of busulfan with oligonucleotides suggested that this agent forms intrastrand cross-links with 5′-GA-3′ sequences.[27]

The structure of the O^6-2′-deoxyguanosine-alkyl-O^6-2′-deoxyguanosine cross-link and the sequences containing the butyl and heptyl cross-links (**XL4** and **XL7**) are shown in Fig. 1. The synthesis of the cross-linked amidites **7a** and **7b** were performed according to the synthetic pathway in Scheme 1. Starting from commercially available 5′-*O*-dimethoxytrityl-N^2-phenoxyacetyl-O^6-2′-deoxyguanosine the free 3′-alcohol was protected as an allyloxycarbonyl ester **1** using allyl 1-benzotriazoyl carbonate.[28] The adducts **2a** and **2b** were prepared by introduction of 1-*tert*-butyldiphenylsilyloxy-butan-4-ol or 1-*tert*-butyldiphenyl silyloxy-heptan-7-ol at the O^6 position of **1** *via* the Mitsunobu reaction.[18,20] Removal of the *tert*-butyldiphenylsilyl protecting group on compounds **2a** and **2b** was accomplished with TBAF at room temperature for 30 min to yield the adducts **3a** and **3b**. The formation of dimers **5a** or **5b** were achieved *via* a second Mitsunobu reaction using 5′-*O*-dimethoxytrityl-3′-*O*-*tert*-butyldimethyl-silyl-2′-deoxyguanosine (**4**) in yields of 63 and 71%, respectively. Amidite precursors **6a** and **6b** required the removal of the 3′-*O*-alloxycarbonyl group from **5a** or **5b** with palladium (0) tetrakistriphenylphosphine in THF at room temperature. These were then converted to phosphoramidites **7a** and **7b** using a slight excess of *N*,*N*-diisopropylamino cyanoethyl phosphonamidic chloride and isolated by hexane precipitation. The isolated phosphoramidites **7a** and **7b** were analyzed by mass

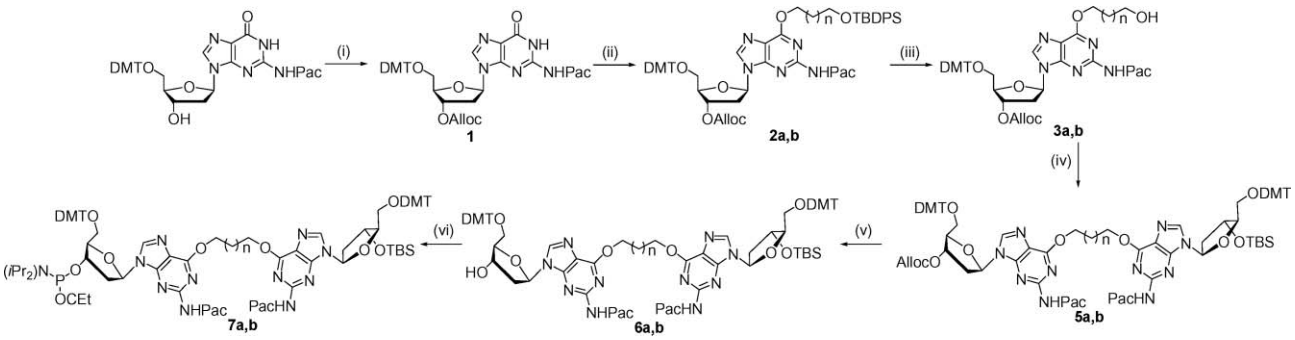

Scheme 1 Synthesis of O^{6}G-alkyl-O^{6}G amidite **7a** ($n = 2$) and **7b** ($n = 5$). (i) Alloc-OBt, CH_2Cl_2/pyridine (9 : 1), 12 h; (ii) 4-(*tert*-butyldiphenylsiloxy) butanol or 7-(*tert*-butyldiphenylsiloxy) heptanol (1.1 eqv.), PPh_3 (1.25 eqv.), DIAD (1.2 eqv.) (iii) TBAF (1 M in THF), 30 min; (iv) **4** (1.01 eqv.), PPh_3 (1.25 eqv.), DIAD (1.2 eqv.), 1 h; (v) $Pd(PPh_3)_4$ (5 mol%), PPh_3 (0.25 eqv.), n-butylamine/formic acid (1 : 1, 2.5 eqv.), THF, 20 min; (vi) *N*,*N*-diisopropylamino cyanoethyl phosphonamidic chloride, DIPEA, THF, 30 min.

spectrometry and were found to have the expected molecular masses. ^{31}P NMR analysis of these phosphoramidites revealed the presence of two signals for **7a** (143.92 and 144.14 ppm) and **7b** (143.91 and 144.11 ppm) in the region diagnostic for a phosphoramidite.

The synthesis of the 1,3-GNC engineered ICL using phosphoramidite dimers **7a** or **7b** required three different protecting groups around the cross-linked site enabling an orthogonal approach for their removal. This would allow for the synthesis of three different branches in terms of sequences around the site of the ICL. The Mitsunobu reaction was chosen for its specificity at the O^6 position of a protected 2′-deoxyguanosine[18,20] and the versatility of this method which allows for the synthesis of cross-links of various lengths, depending on the diol linker used. This reaction was employed twice in the synthetic pathway outlined in Scheme 1, first for the synthesis of the monomers **2a** and **2b** containing the four and seven carbon linkers at the O^6 atom and later in the scheme for dimers **5a** and **5b**. The dimerization reaction to give dimer **5b** proceeded in a slightly higher yield relative to **5a** (71 *versus* 63%), presumably due to the reduced steric hindrance of the longer alkyl linker of **3b** that reacts with **4**.

Solid phase synthesis of **XL4** and **XL7** was performed on a 1 μmol scale using phosphoramidites **7a** or **7b** according to Fig. 2. The first arm of the duplex was synthesized on a polystyrene support using commercially available 3′-*O*-2′-deoxyphosphoramidites. Coupling of the cross-linked phosphoramidites **7a** or **7b** introduced the ICL at the 5′-ends to the linear oligomers. The dimethoxytrityl groups of the dimer moiety were removed by brief treatment with 3% TCA in methylene chloride to expose the 5′-OH groups from which the second and third arms of the duplex were then synthesized with a noted increase in the trityl conductivity reading on the synthesizer. Repetitive coupling with protected 3′-*O*-2′-deoxyphosphoramidites gave, after detritylation and capping (phenoxyacetic anhydride), the branched oligomer **Y-TBS** (Fig. 2). The 3′-*O*-TBS group was then removed from **Y-TBS** by treating the support with anhydrous triethylamine for 16 h followed by TEA·3HF twice for 30 min at room temperature. C-18 Reversed-phase HPLC analysis of the deprotected intermediate **Y-OH** revealed complete removal of the silyl group with the shift of the major peak from 11.2 to 8.2 min in the case of the butyl containing cross-link (see ESI†). Continued synthesis with

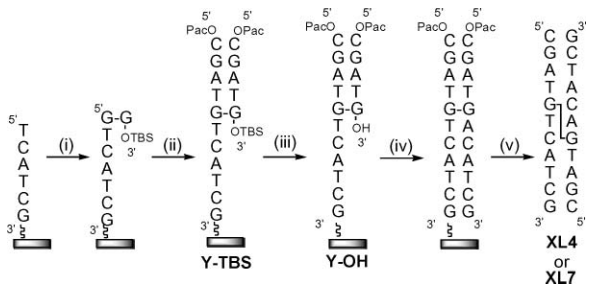

Fig. 2 Methodology to construct the cross-linked duplexes **XL4** and **XL7** *via* solid phase synthesis: (i) coupling of amidite **7a** or **7b**; (ii) extension with 3′-*O*-2′-deoxyphosphoramidites followed by capping with phenoxyacetic anhydride; (iii) removal of the 3′-*O*-*tert*-butyldimethylsilyl group with TEA·3HF; (iv) extension with 5′-*O*-2′-deoxyphosphoramidites and (v) cleavage from the solid support.

repetitive coupling of 5′-*O*-2′-deoxyphosphoramidites at the 3′-end of intermediate **Y-OH** gave full length ICL duplexes **XL4** and **XL7**.

The solid-phase synthesis of the ICL containing oligonucleotides **XL4** and **XL7** required some changes from the standard synthesis cycle and reagents employed during solid-phase oligonucleotide synthesis. First, synthesis was performed using a polystyrene rather than controlled-pore glass (CPG) solid-support due to the incompatibility of TEA·3HF with the latter.[5] As an added precaution, the cyanoethyl protecting groups were removed using TEA as it has been observed that prolonged fluoride treatment using TBAF could lead to chain cleavage.[29] Phenoxyacetic anhydride rather than acetic anhydride was used as capping reagent due to a undesirable *N*-acetylation reaction that has been observed with 'fast-deprotecting' amidites.[30] Additionally, the protection of the exocyclic amine functionalities of the cross-linked guanosine bases with the phenoxyacetyl group would allow for milder deprotection conditions and ease of its removal at the final stage.

Chain assembly in the 3′ to 5′ direction proceeded smoothly using 3′-*O*-deoxyphosphoramidites and the cross-linked dimers **7a** and **7b** with essentially quantitative coupling observed by conductivity measurements to assess the trityl values. A higher

Table 1 Amounts, retention times, nucleoside ratios and mass spectral data for cross-linked duplexes **XL4** and **XL7**

Duplex	A_{260} Units[a]	Retention time[b]	Nucleoside	Ratios exp	Ratios obs	Mass exp	Mass obs
XL4	141.8 (36.9)	23.7	dC	6.0	6.1	6727.5	6726.8
			dG	4.0	4.2		
			dT	5.0	5.0		
			dA	5.0	5.1		
			dG-dG	1.0	1.1		
XL7	108.6 (39.1)	25.5	dC	6.0	5.8	6769.6	6769.0
			dG	4.0	4.1		
			dT	5.0	5.0		
			dA	5.0	5.1		
			dG-dG	1.0	1.1		

[a] Amount of crude ICL duplex purified by SAX HPLC. The numbers in parentheses indicate the amount of pure duplex obtained. [b] Retention times (min) of ICL duplexes on SAX HPLC using a 0.0–0.5 M linear gradient of sodium chloride.

concentration (0.15 M) and longer coupling time (10 min) was used for phosphoramidites **7a** and **7b** to ensure a high coupling efficiency due to their larger size compared to the standard 3′-*O*-deoxyphosphoramidites. At this point, capping with phenoxyacetyl anhydride gave intermediate **Y-TBS** (Fig. 2) which was desilylated to give the free 3′OH functionality. The efficiency of this step was readily monitored by C-18 reversed phase HPLC (see ESI†). A small amount (approximately 1 mg) of the solid support was deprotected using NH_4OH/ethanol (3 : 1), milder conditions that have been developed for the deprotection of RNA to ensure that the TBS groups are not removed.[31] The removal of the TBS group decreases the hydrophobicity of the oligomer and a change in the retention time for the oligomer from 11 to 8 min on the C-18 reverse phase HPLC indicates removal to give the more hydrophilic **Y-OH** intermediate (Fig. 2). The final step in the assembly of **XL4** and **XL7** is continued chain extension with 5′-*O*-2′-deoxyphosphoramidites. Cleavage and deprotection of **XL4** and **XL7** were performed with concentrated ammonium hydroxide/ethanol (3 : 1) at 55 °C for 4 h to yield 141.8 and 108.6 OD of material, respectively (see Table 1). Analysis by SAX HPLC analysis revealed that the major product was the desired ICL whose retention times are shown in Table 1 (see ESI for HPLC traces of crude and purified material†). The combination of mild deprotection conditions and bulky nature of the adduct that the ICL represents at the O^6 position may account for the stability under these deprotection conditions. Purification by SAX HPLC, followed by desalting gave **XL4** and **XL7** in approximately 26 and 36% overall isolated yields.

These ICL duplexes were digested to the constituent nucleosides with a combination of snake venom phosphodiesterase and calf intestinal phosphatase and analyzed by C-18 reversed phase HPLC (see ESI for HPLC traces†). In addition to the four standard 2′-deoxynucleosides, one additional peak was observed with a retention time of 18.1 min for **XL4** and 25.5 min for **XL7**. These additional peaks had retention times identical to completely deprotected dimers of **6a** and **6b**. As shown in Table 1, the ratios of the component 2′-deoxynucleosides and cross-linked nucleosides were consistent with the theoretical composition of ICL duplexes **XL4** and **XL7**. The ICL oligomers **XL4** and **XL7** required additional time for digestion compared to single stranded oligonucleotides (48 h as opposed to 30 min). ESI mass spectrometry of the duplexes **XL4** and **XL7** had masses of 6726.8 and 6769.0 Da, consistent with the theoretical values for the cross-linked duplexes.

UV thermal denaturation and circular dichroism spectra (CD) of ICL duplexes

UV denaturation experiments were carried out to assess the effect of the alkyl linkers on duplex stability. The UV thermal denaturation (T_m) curves for the ICL duplexes **XL4**, **XL7**, and the corresponding non-cross-linked control duplex all exhibited a sigmoidal denaturation profile with similar hyperchromicities for the transition curves (see ESI†). The melting temperature for **XL4**, **XL7** and the non-cross-linked control were all similar with a value of ~48 °C.

When this ICL was present as a directly opposed O^6-2′-deoxyguanosine-heptyl-O^6-2′-deoxyguanosine mismatch in an 11-bp duplex, an increase in T_m of 23 °C over the control duplex was observed.[16] UV thermal denaturation experiments with oligonucleotides containing an O^6-methyl-2′-deoxyguanosine/2′-deoxycytosine base pair have shown that a single O^6-methyl substitution reduced duplex stability by at least 18 °C per substitution in 1 M NaCl buffer and DNA duplexes containing two of these alkylated lesions were found to have a T_m 40 °C lower than that of the unmodified duplex.[32,33,34] It is believed that the destabilizing nature of the O^6-alkyl lesions are counterbalanced by the preorganization of the covalently linked strands of the duplex resulting in a stability comparable to the non-cross-linked control.[5,16]

The CD spectra of cross-linked duplexes **XL4**, **XL7** and the non-cross-linked control were recorded at 10 °C (spectra are shown in ESI†). In all cases, the CD spectra of the duplexes exhibited signatures characteristic of B-form DNA with a positive maximum peak centered around 275 nm, a negative peak at approximately 250 nm and a cross over around 260 nm.[35,36] The CD spectra of non-cross-linked controls revealed some minor differences, particularly a reduction of the signal at 275 nm.

These results suggests that the cross-links had minimal effect on the global B-form structure. NMR studies performed with dodecanucleotides containing a O^6meG·C base pair implicate the formation of a wobble base pair, with the methylated guanine sliding towards the major groove and the cytosine oriented towards the minor groove. This base pair is stacked in the duplex between the flanking base pairs inducing only a small conformational change from the wild-type duplex.[37] In a standard B-form duplex, the distance between the O^6–O^6 atoms in a 5′-GNC sequence is approximately 6.4 Å. The O–O distance in the fully extended 1,4-butanediol and 1,7-heptanediol is 6.2 and 9.9 Å, respectively, which is sufficient to span the distance linking the two O^6 atoms in a 5′-GNC sequence motif without inducing a significant structural change. Molecular models for the oligomers **XL4**, **XL7** and the non-cross-linked control duplex that were geometry optimized using the AMBER forcefield suggest that the alkyl linkers are oriented towards the major groove and do not greatly distort the duplex (see ESI†).

ICL repair assay with hAGT

Repair assays were performed on the ICLs containing oligomers **XL4** and **XL7** with wild-type hAGT and the mutants C145S, P140A and V148L. The C145S mutant was selected as a negative control due to its lack of alkyltransferase activity and for the investigation of protein binding to the O^6-dG-alkyl-O^6-dG ICLs.[38] The P140A mutation has been investigated for the influence of reduced size of the active site pocket on hAGT activity.[39,40] In addition, some AGTs such as the *E.coli* Ada-C, have alanine in place of proline in the equivalent position of hAGT. The V148L mutant was engineered to probe the effect of the side chain of V148 on the repairing ability of the protein. This mutant was selected as little is known about this amino acid other than the carbonyl group of V148 has been shown in wild-type hAGT to accept a H-bond from the N^2 atom of a bound guanine base.[22,41] We suspected that substituting Val to a larger amino acid would reduce the size of the active site pocket yielding a protein with the same properties as P140A.

All protein (wild-type hAGT, C145S, P140A and V148L) masses were verified by ESI-MS and were in agreement with the calculated values (see ESI†). The secondary structure of the proteins by far UV CD was examined to ensure that the mutations did not compromise the structure. CD scans of the P140A and V148L hAGT mutants revealed similar secondary structures to the wild-type hAGT due the highly conservative nature of these mutations (see ESI†). The C145S mutation had a greater impact on the global secondary structure of the protein. Although the size of the cysteine and serine side groups are relatively similar, the H-bonding capabilities of these two amino acids differ.

The stability of the proteins (wild-type hAGT, C145S, P140A and V148L) were assessed *via* thermal denaturation studies to ensure that the proteins were properly folded at the assay temperature (37 °C) by monitoring the α-helical content of the protein at 222 nm as a function of increasing temperature. The thermal denaturation studies demonstrated that all hAGT proteins were still properly folded at 37 °C due to their T_m's being well above 37 °C. Thermal denaturation studies of the wild-type hAGT correlated with values reported for complete inactivation of the protein at 60 °C.[42] All mutations destabilized the protein based on CD spectra where the stability of the secondary structure of the protein was compromised (see ESI†). Presumably, the presence of an additional methylene group in the V148L mutant affected protein stability negatively while the P140A mutant exhibited a smaller entropy increase upon folding for the alanine *versus* proline substitution leading to a reduced protein stability.

The intrinsic fluorescence of the hAGT proteins were investigated by monitoring the local environments containing both tryptophan and tyrosine residues using an excitation wavelength of 280 nm while in the case of tryptophan alone the excitation wavelength of 295 nm was used. It is clear from the emission wavelengths and intensities that the mutations had no dramatic affect on the tertiary structure of the protein with V148L having a slight impact on tertiary structure of the protein relative to the other mutants (see ESI†).

The 5′-^{32}P labeled ICL DNA duplexes **XL4** and **XL7** (2 pmol) were incubated with 60 pmol of either the wild-type hAGT or the mutants (C145S, P140A and V148L) overnight at 37 °C to determine repair. Trials for either 14 or 16 h were performed with virtually identical results obtained, indicating that the reaction was complete as monitored by denaturing PAGE (Fig. 3). Lanes 1 and 2 contain 2 pmol of ssDNA corresponding to the sequence of one of the repaired strands with the only difference being the presence of hAGT in lane 2. Lanes 3 and 8 contain 2 pmol of **XL4** and **XL7**, respectively, representing the unrepaired ICL duplexes with a reduced mobility relative to that of completely repaired substrate. Lanes 4 and 9 contain 60 pmol of hAGT with 2 pmol of either **XL4** (lane 4) or **XL7** (lane 9). In both cases two additional bands are seen, one that migrates more quickly corresponding to the completely repaired single stranded product and the other at the top of the gel with significantly reduced mobility which is likely a single hAGT-bound covalently to a DNA species, a median repair product. For both **XL4** and **XL7**, no repair products are observed with 60 pmol of the mutants C145S (lanes 5 and 10), while P140A (lanes 6 and 11) or V148L (lanes 7 and 12) show very minimal repair of **XL7** and no repair of **XL4**. The repair assays demonstrate that both **XL4** and **XL7** are repaired by hAGT with **XL7** undergoing a greater amount of repair (with 57.0% of ICLs repaired) over **XL4** (31.4% of ICLs repaired) based on quantitation of ICLs remaining as measured by the relative counts of the labelled products present on the gel by ImageQuant™ (see ESI†).

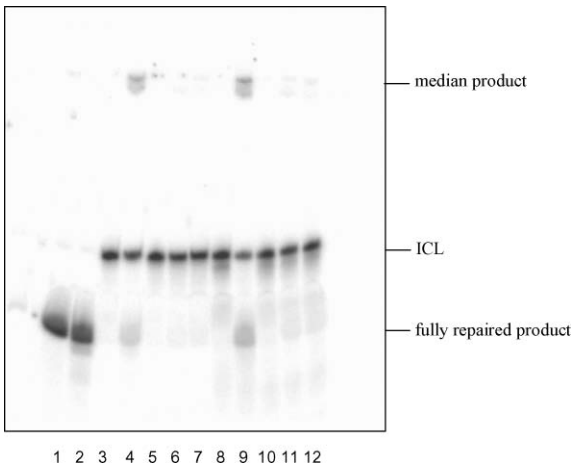

Fig. 3 Repair of **XL4** and **XL7** by wild-type hAGT, C145S, P140A and V148L. Denaturing PAGE of repair reactions as described in the experimental section: Lane 1, 2 pmol Control; lane 2, 2 pmol Control + 60 pmol hAGT; lane 3, 2 pmol **XL4**; lane 4, 2 pmol **XL4** + 60 pmol hAGT; lane 5, 2 pmol **XL4** + 60 pmol C145S; lane 6, 2 pmol **XL4** + 60 pmol P140A; lane 7, 2 pmol **XL4** + 60 pmol V148L; lane 8, 2 pmol **XL7**; lane 9, 2 pmol **XL7** + 60 pmol hAGT; lane 10, 2 pmol **XL7** + 60 pmol C145S; lane 11, 2 pmol **XL7** + 60 pmol P140A; lane 12, 2 pmol **XL7** + 60 pmol V148L.

For the repair assays involving **XL4** and **XL7**, the samples were denatured in stop reaction buffer before being loaded on a 7 M urea denaturing gel to prevent self-complexation of the repaired DNA strands which could complicate determination of ratios of the repaired intermediate and fully repaired product *versus* intact (unrepaired) ICLs (Scheme 2).

The inactive C145S mutant was unable to repair both ICL duplexes as expected due to the lack of the active site Cys residue which is known to be the alkyl group acceptor. The other P140A and V148L mutants showed no repair of **XL4** and very poor

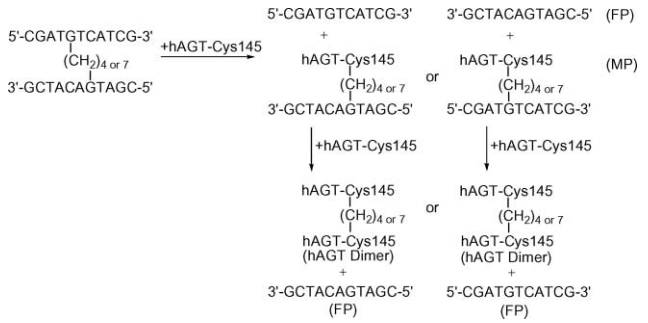

Scheme 2 Proposed repair pathway of cross-link species by wild-type hAGT, P140A and V148L (MP - median product; FP- final product).

repair for **XL7** (4.5% and 3.0%, respectively). The diminished capacity for repair by the P140A mutant has been observed as it is much less active than wild-type hAGT in dealkylating O^6-benzylguanine, which has been explained by the reduced size of the binding pocket.[43]

Time course assays were performed using 60 pmol wild-type hAGT and 2 pmol of the **XL4** and **XL7** substrates by quantitating the amount of unrepaired, partially and fully repaired species (see ESI†). **XL4** was repaired at a much slower rate with 25% repair of the ICLs occurring in 8.5 h whereas the same level of repair for **XL7** required approximately 1 h.

The results obtained from the time course experiments for the 5′-GNC-3′ ICLs for **XL4** and **XL7** follow similar trends to repair results for the directly opposed O^6-dG-alkyl-O^6-dG ICL in a mismatch duplex.[44] It was shown that 50% final product was formed after 2 h for a directly opposed O^6-dG-heptyl-O^6-dG mismatch ICL, also observed in the repair of **XL7**. These results are surprising, as the ICL spanning a 5′-GNC-3′ motif would be expected to be a less flexible substrate relative to directly opposed O^6-dG-heptyl-O^6-dG mismatch ICLs. The mechanism by which hAGT repairs DNA alkylation involves rotation of the alkylated base from the DNA duplex from the minor groove into the active site allowing for transfer of the alkyl group to the residue C145.[21] The improved repair of **XL7** *versus* **XL4** can be rationalized by the difference in distances of the cross-link. For the four carbon linker of **XL4**, the O–O distance of the fully extended linker is just sufficient (6.2 Å) to span the distance necessary to link the O^6 atoms in a 5′-GNC sequence (6.4 Å). In a geometry optimized model of **XL4**, the O–O distance was found to be 4.5 Å with some tilting of the guanine bases towards each other (see ESI†). The model of **XL7** has an O–O distance of 7.1 Å with the longer alkyl chain protruding into the major groove. This would suggest that rotation of one of the alkylated guanines of **XL7** into the active site of hAGT would be less difficult relative to the more strained **XL4** ICLs. These findings demonstrate that there could have been some distortion in the cross-linked duplexes inherent in the nature of the substrates prior to the repair process and that **XL4** is too short to fit optimally in the active site relative to the **XL7** counterpart.

The formation of the final product occurs at a faster rate than the formation of the median product for both **XL4** and **XL7**, as the % final product observed is always greater than the % median product. Final and median product formation occur at different rates, suggesting that hAGT preferentially repairs the median product over the initial substrate as indicated by the lack of accumulation of median product at any time. If hAGT preferentially repaired the median product over the initial substrate the median product should not increase with time as the median product would be consumed as it would be formed.

One possible explanation as to why this reaction does not go to completion is that the reacted hAGT binds to another lesion containing ICLs or oligonucleotide in our assay. It is known that alkylated hAGT can also bind to DNA.[45] *In vivo*, dissociation is most likely reinforced by ubiquitination resulting in degradation of the alkylated hAGT.[46] In addition, it is possible that the cross-link may be oriented in an alternate, less reactive conformation, as has been postulated for O^6-(2-hydroxyethyl)guanine and O^6-[4-oxo-4-(3-pyridyl)but-1-yl]guanine containing oligonucleotides.[47]

Table 2 Hill factor and monomeric K_d values of C145S hAGT-DNA complexes

DNA	Cooperativity Factor	K_d/μM
Control	1.41 ± 0.06	8.36 ± 1.11
XL4	1.75 ± 0.13	9.87 ± 1.22
XL7	1.32 ± 0.06	9.67 ± 1.12

Binding studies of C145S hAGT mutant using protein titration

Binding cooperativity (Hill factor) and monomeric K_d values were determined for the non-cross-linked control duplex, **XL4** and **XL7** with the C145S hAGT mutant (see Table 2 and ESI†). Similar cooperativity values were obtained for the control duplex (1.41 ± 0.06) and **XL7** (1.32 ± 0.06) whereas this value was found to be slightly higher for **XL4** (1.75 ± 0.13). All three DNA duplexes showed a similar monomeric dissociation constant ranging from 8.36 for the control duplex to 9.87 μM for **XL4** (see ESI).

Experiments to measure cooperativity and dissociation constants for **XL4** and **XL7** showed only two bands by EMSA corresponding to the free and bound ICL DNA. The absence of an intermediate band on the native gel indicates that there is cooperativity in the binding of hAGT for the ICL DNA. **XL7** and the control duplex showed similar cooperativity and dissociation constants indicating that the presence of the 7-methylene cross-link had little influence on hAGT interaction with the DNA. **XL4** had a slightly higher cooperativity of interaction with hAGT, however, all the measured Hill factors for ICL duplexes **XL4** and **XL7** were between 1 and 2 in accordance with previous work which showed that 1 hAGT protein binds every 4 nucleotides.[48] A stoichiometry value of 2 indicates perfect cooperativity, as previously shown in the case of hAGT for many oligonucleotide sequences under different assay conditions whereas a value of 1 indicates no cooperativity.[48]

In the absence of NMR or X-ray structural data for **XL4** or **XL7**, it can only be speculated that the 4-methylene cross-link induces a structural change in the DNA that has an influence on the interaction of the ICL with hAGT contributing to the slight increase in cooperativity that is observed. It is known that binding of hAGT to DNA causes structural changes in the DNA, which may play a role in aiding the rotation of the damage base from the DNA double helix and subsequently promote hAGT cooperative binding.[22,49] However, the shorter alkyl linker of **XL4** *versus* **XL7** may hinder rotation of the alkylated guanine into the active site contributing to a reduction in repair by hAGT.

Colony forming assay in CHO cells treated with busulfan and hepsulfam and relevance with O⁶-dG-alkyl-O⁶-dG ICLs

CHO cells that do not express AGT were very sensitive to killing by hepsulfam (Fig. 4). Expression of hAGT provided a significant but not complete protection from this agent. This is consistent with the concept that an O⁶-2′-deoxyguanosine-alkyl-O⁶-2′-deoxyguanosine cross-link accounts for at least part of the cytotoxicity of this agent and that the efficient repair of this 7 carbon adduct by hAGT prevents this killing. There was no protection from busulfan, which is in accordance with the poor repair of the 4 carbon adduct produced by this agent.

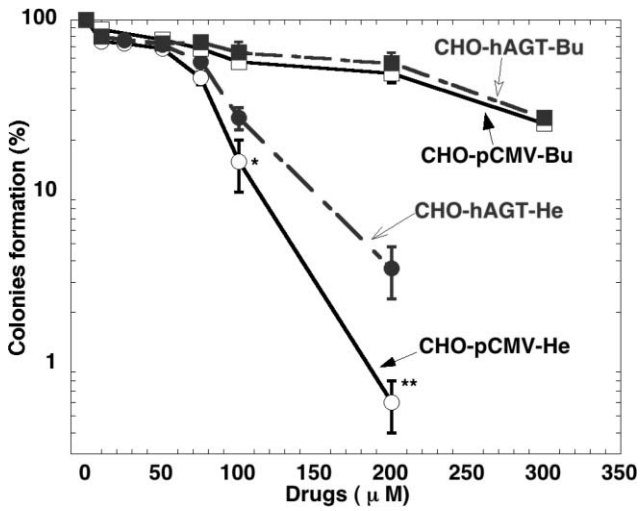

Fig. 4 The effect of the expression of hAGT on sensitivity of CHO cells to busulfan and hepsulfam. Cell survival was measured with a colony forming assay as described in the Experimental section. * $p<0.05$, Compared to cells expressing hAGT; ** $p<0.01$, Compared to cells expressing hAGT.

Extensive study of the hAGT reaction has shown that DNA repair by this protein is specific for adducts on the O⁶-position with a minor capability to repair adducts on the O⁴-position of thymine. The results shown here using *in vitro* assays show that a DNA interstrand cross-link containing 7 carbon atoms linking two O⁶-2′-deoxyguanosine residues is efficiently repaired by hAGT. Such a cross-link would be expected to be formed in treated cells by hepsulfam and, although it has not yet been characterized, the finding that hAGT reduces the cytotoxicity of hepsulfam is strong evidence that it does occur. Unrepaired DNA interstrand cross-links are very toxic and only a small number of such cross-links may be formed. The results also suggest that a high level of hAGT expression would render tumor cells resistant to therapy with hepsulfam.

Conclusions

The synthesis of nucleoside dimers containing a O⁶-2′-deoxyguanosine-alkyl-O⁶-2′-deoxyguanosine cross-link that enables the construction of a 1,3-staggered 5′-GNC motif by solid-phase synthesis using phosphoramidite chemistry and an orthogonal approach to removing protecting groups is described. These ICLs were obtained in high yield and purity that is required for DNA repair studies. ICL duplexes containing a four and seven methylene linkage were found to have similar thermal stability and structure relative to a non-cross-linked control. Both were also repaired by hAGT, with efficiency higher for the ICLs containing the seven methylene linkage. Binding studies suggested similar affinity of hAGT for both ICLs. Studies with cells treated with hepsulfam demonstrate that hAGT reduces the cytotoxicity this bifunctional alkylating agent induces and serves as evidence that the O⁶-2′-deoxyguanosine-alkyl-O⁶-2′-deoxyguanosine cross-link may account for at least part of the cytotoxicity of this agent.

Experimental

5′-*O*-Dimethoxytrityl-N²-phenoxyacetyl-2′-deoxyguanosine, 3′-*O*-dimethoxytrityl-2′-deoxyribonucleoside-5′-*O*-(β-cyanoethyl-*N*,*N*′-diisopropyl) phosphoramidites and N,N-diisopropylamino cyanoethyl phosphonamidic chloride were purchased from ChemGenes Inc. (Wilmington, MA). 5′-*O*-Dimethoxytrityl-2′-deoxyribonucleoside-3′-*O*-(β-cyanoethyl-*N*,*N*′-diisopropyl)-phosphoramidites and protected 2′-deoxyribonucleoside-polystyrene supports were purchased from Glen Research (Sterling, Virginia). All other chemicals and solvents were purchased from the Aldrich Chemical Company (Milwaukee, WI) or EMD Chemicals Inc. (Gibbstown, NJ). Flash column chromatography was performed using silica gel 60 (230–400 mesh) obtained from Silicycle (Quebec City, QC). Thin layer chromatography (TLC) was performed using precoated TLC plates (Merck, Kieselgel 60 F_{254}, 0.25 mm) purchased from EMD Chemicals Inc. (Gibbstown, NJ). NMR spectra were recorded on a Varian INOVA 300 MHz NMR spectrometer at room temperature. ^{1}H NMR spectra were recorded at a frequency of 300.0 MHz and chemical shifts were reported in parts per million downfield from tetramethylsilane. ^{31}P NMR spectra (^{1}H decoupled) were recorded at a frequency of 121.5 MHz with H_3PO_4 used as an external standard. ESI mass spectra for oligonucleotides were obtained at the Concordia University Centre for Biological Applications of Mass Spectrometry (CBAMS) using a Micromass Qtof2 mass spectrometer (Waters) equipped with a nanospray ion source. The mass spectrometer was operated in full scan, negative ion detection mode. ESI mass spectra for small molecules were recorded at the McGill University Department of Chemistry Mass Spectrometry Facility with a Finnigan LCQ DUO mass spectrometer in methanol or acetone. Ampicillin, isopropyl β-D-thiogalactopyranoside (IPTG), and most other biochemical reagents as well as polyacrylamide gel materials were purchased from Bioshop Canada Inc (Burlington, ON). Ni-NTA Superflow Resin was purchased from Qiagen (Mississauga, ON). Complete, Mini, EDTA-free Protease Inhibitor Cocktail Tablets were obtained from Roche (Laval, QC) Nitrocellulose filters (0.20 μm) were obtained from Millipore. XL-10 Gold *E. coli* cells were obtained from Stratagene (Cedar Creek, TX). DpnI, T4 polynucleotide kinase (PNK), Unstained Protein Molecular Weight Marker and restriction enzymes EcoRI and KpnI were obtained from Fermentas (Burlington, ON). [γ-^{32}P]ATP was purchased from Amersham Canada Ltd. (Oakville, ON).

3′-*O*-alloxycarbonyl-5′-*O*-dimethoxytrityl-N²-phenoxyacetyl-2′-deoxyguanosine (1)

To a solution of 5′-*O*-dimethoxytrityl-N²-phenoxyacetyl-2′-deoxyguanosine (2.15 g, 3.06 mmol) in anhydrous THF/pyridine

(9 : 1) was added a catalytic amount of dimethylaminopyridine (~ 1 mg) followed by allyl 1-benzotriazoyl carbonate (0.88 g, 4.05 mmol) and the mixture was stirred at room temperature for 24 h. The solvent was removed *in vacuo*, the crude taken up in CH_2Cl_2 (50 mL) and washed twice with 5% sodium bicarbonate (50 mL). The organic layer was then dried over sodium sulfate and evaporated to near dryness. The crude compound was then purified by silica gel column chromatography using a gradient of CH_2Cl_2–methanol (100 : 0.5 → 100 : 1.4) to yield 1.84 g (76.2%) of **1** as a colorless foam. R_f (SiO_2): 0.37 in CH_2Cl_2–MeOH (20 : 1). ^{1}H NMR (300 MHz, $CDCl_3$, ppm): 11.79 (s, 1H, NH), 8.99 (s, 1H, NH), 7.85 (s, 1H, H8), 7.35–7.44 (m, 4H, Ar), 7.18–7.35 (m, 9H, Ar), 7.12 (t, 1H, Ar), 7.02 (dd, 2H, Ar), 6.82 (dd, 4H, Ar), 6.32 (dd, 1H, H1′, J = 6.0), 5.90–6.05 (m, 1H, allyl), 5.31–5.40 (m, 2H, allyl), 4.44–4.50 (m, 1H, H3′), 4.69 (d, 2H, $PhOCH_2CO$), 4.67 (d, 2H, $vinylCH_2CO$), 4.31–4.36 (m, 1H, H4′), 3.79 (s, 6H, OCH_3), 3.35–3.51 (dd, 2H, H5′, H5′), 2.83–2.88 (m, 1H, H2′), 2.64–2.70 (m, 1H, H2′). MS (ESI): *m*/*z* calcd for $C_{43}H_{42}N_5O_{10}[M+H]^+$, 788.3; found, 788.3.

3′-*O*-alloxycarbonyl-5′-*O*-dimethoxytrityl-N^2-phenoxyacetyl-O^6-(4-*tert*-butyldiphenylsiloxybutyl)-2′-deoxyguanosine (2a)

To a solution of **1** (5.37 g, 6.82 mmol) in anhydrous dioxane (40 mL) was added 1-*tert*-butyldiphenylsilylbutanol (1.97 g, 9.63 mmol) and triphenylphosphine (2.55 g, 9.72 mmol) followed by the dropwise addition of diisopropylazodicarboxylate (1.89 g, 9.34 mmol) introduced in dioxane (4.4 mL). The solvent was evaporated after 1 h and the crude was taken up in CH_2Cl_2 (50 mL) and washed twice with 5% sodium bicarbonate (50 mL). The organic layer was then dried over magnesium sulfate, filtered and evaporated. The crude compound was purified by silica gel column chromatography using a gradient of hexanes/ethyl acetate (19 : 1 → 13 : 7). Triphenylphosphine oxide was precipitated from contaminated fractions with diethyl ether and separated by filtration. Evaporation of the solvent afforded 5.16 g (78.8%) of the compound as a colorless foam. R_f (SiO_2): 0.67, hexanes/ethylacetate 2 : 3. ^{1}H NMR (300 MHz, DMSO-d_6, ppm): 10.52 (s, 1H, NH), 8.36 (s, 1H, H8); 7.34–7.64 (m, 11H, Ar); 7.11–7.29 (m, 11H, Ar); 6.89–6.95 (m, 3H, Ar); 6.65–6.74 (dd, 4H, Ar); 6.40 (dd, 1H, H1′, J = 7.2); 5.84–5.98 (m, 1H, allyl); 5.20–5.35 (m, 3H, allyl, H3′); 4.97–5.06 (m, 2H, CH_2OAr); 4.50–4.64 (m, 4H, $vinylCH_2CO$, $PhOCH_2CO$); 4.18–4.24 (m, 1H, H4′); 3.70 (t, 2H, CH_2OSi); 3.67 (s, 3H, OCH_3); 3.66 (s, 3H, OCH_3); 3.46 (dd, 1H, H5′); 3.23–3.27 (m, 1H, H2′); 3.15 (dd, 1H, H5′); 2.58–2.63 (m, 1H, H2′); 1.90 (q, 2H, CH_2); 1.67–1.76 (m, 2H, CH_2); 0.94 (s, 9H, $SiC(CH_3)_3$). MS (ESI): *m*/*z* calcd for $C_{63}H_{67}N_5O_{11}SiNa$ $[M+Na]^+$, 1062.5, found 1062.4.

3′-*O*-alloxycarbonyl-5′-*O*-dimethoxytrityl-N^2-phenoxyacetyl-O^6-(7-*tert*-butyldiphenylsiloxyheptyl)-2′-deoxyguanosine (2b)

To a solution of **1** (3.48 g, 4.41 mmol) in anhydrous dioxane (20 mL) was added 1-*tert*-butyldiphenylsilyloxyheptanol (1.80 g, 4.86 mmol) and triphenylphosphine (1.76 g, 6.71 mmol) followed by diisopropylazodicarboxylate (1.37 g, 6.46 mmol) introduced dropwise in dioxane (1.6 mL). The solvent was evaporated after 1 h and the crude was taken up in CH_2Cl_2 (50 mL) and washed twice with 5% sodium bicarbonate (50 mL). The organic layer was then dried over magnesium sulfate, filtered and evaporated to a solid. The crude compound was purified by silica gel column chromatography using a gradient of hexanes/ethyl acetate (19 : 1 → 13 : 7). Triphenylphosphine oxide was precipitated from contaminated fractions with diethyl ether and separated by filtration. Evaporation of the solvent afforded 3.08 g (61.9%) of the product as a colorless foam. R_f (SiO_2): 0.67, hexanes/ethylacetate 2 : 3. ^{1}H NMR (300 MHz, $CDCl_3$, ppm): 8.68 (s, 1H, NH); 8.10 (s, 1H, H8); 7.66–7.71 (m, 4H, Ar); 7.16–7.46 (m, 18H, Ar); 7.01–7.10 (m, 3H, Ar); 6.79 (dd, 4H, Ar); 6.48 (dd, 1H, H1′, J = 5.7); 5.89–6.04 (m, 1H, allyl); 5.30–5.46 (m, 2H, allyl); 4.47–4.52 (m, 1H, H3′); 4.78 (s, 2H, CH_2OAr); 4.67 (dt, 2H, $vinylCH_2CO$); 4.59 (d, 2H, $PhOCH_2CO$); 4.35–4.39 (m, 1H, H4′); 3.78 (s, 6H, OCH_3); 3.67 (t, 2H, CH_2OSi); 3.52 (dd, 1H, H5′); 3.41 (dd, 1H, H5′); 3.18–3.23 (m, 1H, H2′); 2.71–2.76 (m, 1H, H2′); 1.89 (q, 2H, CH_2); 1.33–1.62 (m, 6H, $(CH_2)_3$); 1.06 (s, 9H, $SiC(CH_3)_3$). MS (ESI): *m*/*z* calcd $C_{66}H_{73}N_5O_{11}SiNa$ $[M+Na]^+$, 1120.5, found 1120.4.

3′-*O*-alloxycarbonyl-5′-*O*-dimethoxytrityl-N^2-phenoxyacetyl-O^6-(4-hydroxybutyl)-2′-deoxyguanosine (3a)

To a solution of **2a** (5.15 g, 5.38 mmol) in anhydrous THF (10 mL) was added dropwise tetrabutylammonium fluoride (1 M in THF, 645 µL, 6.45 mmol) and the solution was stirred at room temperature for 30 min. On completion the reaction was concentrated, taken up in CH_2Cl_2 (50 mL), washed twice with 5% sodium bicarbonate (50 mL), the organic layer dried over sodium sulfate and evaporated to dryness. The crude was purified by silica gel column chromatography using a gradient of hexanes/ethyl acetate (60 : 40 → 20 : 80) to yield 3.25 g (70.3%) of product as a colorless foam. R_f (SiO_2): 0.50, CH_2Cl_2–MeOH 10 : 1. ^{1}H NMR (300 MHz, DMSO-d_6, ppm): 10.58 (s, 1H, NH), 8.41 (s, 1H, H8); 7.31–7.36 (m, 4H, Ar); 7.18–7.21 (m, 7H, Ar); 6.95–7.02 (m, 3H, Ar); 6.71–6.81 (dd, 4H, Ar); 6.45 (dd, 1H, H1′, J = 6.9); 5.89–6.04 (m, 1H, allyl); 5.27–5.41 (m, 3H, H3′, allyl); 4.87–5.15 (m, 2H, CH_2OAr); 4.63–4.67 (dt, 2H, $vinylCH_2CO$); 4.59 (d, 2H, $PhOCH_2CO$); 4.53 (t, 1H, OH); 4.23–4.30 (m, 1H, H4′); 3.74 (s, 3H, OCH_3); 3.73 (s, 3H, OCH_3); 3.44–3.55 (m, 3H, CH_2OH, H5′); 3.26–3.35 (m, 1H, H5′); 3.20 (dd, 1H, H2′); 2.57–2.69 (m, 1H, H2′); 1.90 (q, 2H, CH_2); 1.56–1.68 (m, 2H, CH_2). MS (ESI): *m*/*z* calcd for $C_{47}H_{49}N_5O_{11}Na$ $[M+Na]^+$, 882.3, found 882.2.

3′-*O*-alloxycarbonyl-5′-*O*-dimethoxytrityl-N^2-phenoxyacetyl-O^6-(7-hydroxyheptyl)-2′-deoxyguanosine (3b)

To a solution of **2b** (1.35 g, 1.20 mmol) in anhydrous THF (10 mL) was added dropwise tetrabutylammonium fluoride (1 M in THF, 135 µL, 1.35 mmol) and the solution was stirred at room temperature for 30 min. On completion the reaction was concentrated, taken up in CH_2Cl_2 (50 mL) and washed twice with 5% sodium bicarbonate (50 mL). The organic layer was then dried over sodium sulfate, evaporated and the crude was purified by silica gel column chromatography using a gradient of hexanes/ethyl acetate (60 : 40 → 20 : 80) to yield 0.949 g (89.6%) of a colorless foam. R_f (SiO_2): 0.50, CH_2Cl_2–MeOH 10 : 1. ^{1}H NMR (300 MHz, DMSO-d_6, ppm): 10.55 (s, 1H, NH), 8.36 (s, 1H, H8); 7.23–7.33 (m, 4H, Ar); 7.10–7.20 (m, 7H, Ar); 6.88–6.98 (m, 3H,

Ar); 6.71 (dd, 4H, Ar); 6.40 (dd, 1H, H1′, J = 5.7); 5.85–6.00 (m, 1H, allyl); 5.31–5.39 (m, 1H, H3′); 5.22–5.35 (m, 2H, allyl); 5.00 (t, 2H, CH_2OAr); 4.60 (d, 2H, vinylCH_2CO); 4.52 (d, 2H, PhOCH_2CO); 4.34 (s, 1H, CH_2OH); 4.18–4.26 (m, 1H, H4′); 3.69 (s, 6H, OCH_3); 3.42 (dd, 1H, H5′); 3.30–3.41 (m, 2H, CH_2OH); 3.19–3.31 (m, 1H, H2′); 3.14 (dd, 1H, H5′); 2.56–2.64 (m, 1H, H2′); 1.80 (q, 2H, CH_2CH_2OAr); 1.21–1.47 (m, 6H, $(CH_2)_3$). MS (ESI): *m/z* calcd for $C_{50}H_{55}N_5O_{11}Na$ $[M+Na]^+$, 924.4, found 924.4.

3′-*O*-*tert*-butyldimethylsilyl-5′-*O*-dimethoxytrityl-N²-phenoxyacetyl-2′-deoxyguanosine (4)

To a solution of 5′-*O*-dimethoxytrityl-N²-phenoxyacetyl-2′-deoxyguanosine (1.73 g, 2.46 mmol) in anhydrous *N*,*N*-dimethylformamide was added imidazole (1.13 g, 16.64 mmol) followed by *tert*-butyldimethylsilyl chloride (1.24 g, 8.23 mmol) and the mixture was stirred at room temperature for 16 h. The solvent was removed, and the crude taken up in CH_2Cl_2 (25 mL) and washed twice with 5% sodium bicarbonate (25 mL). The organic layer was then dried over sodium sulfate and evaporated. The crude was purified by silica gel column chromatography using a gradient of hexanes/ethyl acetate (5 : 1 → 1 : 3) to yield 1.58 g (83.2%) of the product which was a colorless foam. R_f (SiO_2): 0.55, CH_2Cl_2–MeOH 10 : 0.8. ^{1}H NMR (300 MHz, DMSO-d_6, ppm): 11.85 (s, 1H, NH), 11.78 (s, 1H, NH), 8.19 (s, 1H, H8); 7.10–7.36 (m, 12H, Ar); 6.92–7.02 (m, 3H, Ar); 6.74–6.84 (t, 3H, Ar); 6.21 (dd, 1H, H1′, J = 6.9); 4.85 (d, 2H, PhOCH_2CO); 4.49–4.54 (m, 1H, H3′); 3.81–3.86 (m, 1H, H4′); 3.70 (s, 6H, OCH_3); 3.05–3.23 (dd, 2H, H5′, H5′); 2.72–2.77 (m, 1H, H2′); 2.32–2.37 (m, 1H, H2′); 0.79 (s, 9H, $SiC(CH_3)_3$); 0.03 (s, 3H, $SiCH_3$); –0.04 (s, 3H, $SiCH_3$). MS (ESI): *m/z* calcd for $C_{45}H_{51}N_5O_8SiNa$ $[M+Na]^+$, 840.3, found 840.2.

1-{O⁶-[3′-*O*-alloxycarbonyl-5′-*O*-dimethoxytrityl-N²-phenoxyacetyl-2′-deoxyguanidyl]}-4-{O⁶-[3′-*O*-*tert*-butyldimethylsilyl-5′-*O*-dimethoxytrityl-N²-phenoxyacetyl-2′-deoxyguanidyl]}-butane (5a)

To a solution of compound **3a** (1.70 g, 1.98 mmol) in anhydrous dioxane (15 mL) was added triphenylphosphine (0.81 g, 3.09 mmol) and compound **4** (1.56 g, 1.93 mmol). Then, diisopropylazodicarboxylate (0.64 g, 3.02 mmol) was introduced in a solution of dioxane (5 mL). The solvent was evaporated after 14 h and the crude was taken up in CH_2Cl_2 (50 mL) and washed twice with 5% sodium bicarbonate (50 mL). The organic layer was then dried over magnesium sulfate and evaporated to dryness, and then purified by silica gel column chromatography using a gradient of hexanes/ethyl acetate (1 : 0 → 1 : 5) to yield 2.07 g (63.1%) of product which was a colorless foam. R_f (SiO_2): 0.45, CH_2Cl_2–MeOH 20 : 1. ^{1}H NMR (300 MHz, $CDCl_3$, ppm): 8.82 (s, 1H, NH); 8.78 (s, 1H, NH); 8.06 (s, 1H, H8); 8.00 (s, 1H, H8); 6.67–7.45 (m, 22H, Ar); 6.94–6.09 (m, 6H, Ar); 6.64–6.80 (m, 8H, Ar); 6.42 (m, 2H, 2 × H1′); 5.86–6.02 (m, 1H, allyl); 5.43–5.51 (m, 1H, H3′); 5.27–5.44 (m, 2H, allyl); 4.78 (s, 4H, CH_2OAr); 4.71 (d, 4H, PhOCH_2CO); 4.57–4.69 (m, 2H, vinylCH_2CO); 4.52–4.64 (m, 1H, H3′); 4.31–4.39 (m, 1H, H4′); 4.03–4.11 (m, 1H, H4′); 3.75 (s, 12H, OCH_3); 3.30–3.56 (m, 4H, 2 × H5′, 2 × H5′); 3.00 (m, 1H, H2′); 2.62–2.76 (m, 2H, H2′, H2′); 2.38–2.49 (m, 1H, H2′); 2.13 (m, 4H, $(CH_2)_2$); 0.85 (s, 9H, $SiC(CH_3)_3$); 0.04 (s, 3H, $SiCH_3$); 0.00 (s, 3H, $SiCH_3$). MS (ESI): *m/z* calcd for $C_{92}H_{98}N_{10}O_{18}SiNa$ $[M+Na]^+$, 1681.7, found 1681.5.

1-{O⁶-[3′-*O*-alloxycarbonyl-5′-*O*-dimethoxytrityl-N²-phenoxyacetyl-2′-deoxyguanidyl]}-7-{O⁶-[3′-*O*-*tert*-butyldimethylsilyl-5′-*O*-dimethoxytrityl-N²-phenoxyacetyl-2′-deoxyguanidyl]}-heptane (5b)

To a solution of **3b** (1.73 g, 1.92 mmol) in anhydrous dioxane (10.0 mL) was added triphenylphosphine (0.77 g, 2.91 mmol) and compound **4** (1.54 g, 1.88 mmol). Then diisopropylazodicarboxylate (0.59 g, 2.78 mmol) was introduced dropwise in a solution of dioxane (3 mL). After 30 min the solvent was evaporated, the crude was taken up in CH_2Cl_2 (50 mL) and washed twice with 5% sodium bicarbonate (50 mL). The organic layer was then dried over sodium sulfate and evaporated to dryness. The crude was purified by silica gel column chromatography using a gradient of hexanes/ethyl acetate (1 : 0 → 1 : 4) to yield 2.32 g (71.1%) of a colorless foam. R_f (SiO_2): 0.70, CH_2Cl_2–MeOH 10 : 1. ^{1}H NMR (300 MHz, DMSO-d_6, ppm): 10.58 (s, 1H, NH); 10.53 (s, 1H, NH); 8.39 (s, 1H, H8); 8.35 (s, 1H, H8); 7.10–7.34 (m, 22H, Ar); 6.88–6.97 (m, 6H, Ar); 6.64–6.80 (m, 8H, Ar); 6.40 (dd, 1H, H1′, J = 6.0); 6.34 (dd, 1H, H1′, J = 6.6); 5.85–6.00 (m, 1H, allyl); 5.31–5.39 (m, 1H, H3′); 5.21–5.35 (m, 2H, allyl); 4.97–5.03 (m, 4H, PhOCH_2CO); 4.61–4.72 (m, 1H, H3′); 4.60 (d, 2H, vinylCH_2CO); 4.34 (d, 4H, CH_2OAr); 4.17–4.26 (m, 1H, H4′); 3.69–3.77 (m, 1H, H4′); 3.68 (s, 12H, OCH_3); 3.46 (dd, 1H, H5′); 3.10–3.32 (m, 4H, H2′, H5′, 2 × H5′); 2.86–2.98 (m, 1H, H2′); 2.54–2.65 (m, 1H, H2′); 2.27–2.38 (m, 1H, H2′); 1.80 (m, 4H, CH_2CH_2OAr); 1.41; (m, 6H, $(CH_2)_3$); 0.78 (s, 9H, $SiC(CH_3)_3$); 0.00 (s, 3H, $SiCH_3$); –0.05 (s, 3H, $SiCH_3$). MS (ESI): *m/z* calcd for $C_{94}H_{104}N_{10}O_{18}SiNa$ $[M+Na]^+$, 1723.7, found 1724.5.

1-{O⁶-[3′-*O*-*tert*-butyldimethylsilyl-5′-*O*-dimethoxytrityl-N²-phenoxyacetyl-2′-deoxyguanidyl]}-4-{O⁶-[5′-*O*-dimethoxytrityl-N²-phenoxyacetyl-2′-deoxyguanidyl]}-butane (6a)

To a solution of **5a** (0.97 g, 0.59 mmol) in anhydrous THF (3 mL) was added triphenylphosphine (23.0 mg, 0.09 mmol), palladium (0) tetrakistriphenylphosphine (34.0 mg, 0.03 mmol) and a butylamine/formic acid solution (1 : 1, 1.17 mmol) in THF (1 mL). After stirring the mixture for 30 min the reaction was concentrated *in vacuo* and the crude taken up in CH_2Cl_2 (25 mL) and washed twice with 5% sodium bicarbonate (25 mL). The organic layer was dried over sodium sulfate, filtered and evaporated. The crude was purified by silica gel column chromatography using a gradient of hexanes/ethyl acetate (3 : 7 → 1 : 9) to give 0.87 g (94.4%) of colorless product. R_f (SiO_2): 0.41 hexanes/ethyl acetate (1 : 9). ^{1}H NMR (300 MHz, DMSO-d_6, ppm): 10.65 (s, 2H, NH); 8.45 (s, 1H, H8); 8.41 (s, 1H, H8); 7.21–7.38 (m, 22H, Ar); 7.03–6.96 (m, 6H, Ar); 6.76–6.85 (m, 8H, Ar); 6.40–6.49 (m, 2H, 2 × H1′); 5.40 (d, 1H, 3′OH); 5.07 (s, 4H, 2 × PhOCH_2CO); 4.64–4.76 (m, 5H, H3′, 2 × CH_2CH_2OAr); 4.52–4.60 (m, 1H, H3′); 4.02–4.07 (m, 1H, H4′); 3.80–3.93 (m, 1H, H4′); 3.76 (s, 12H, OCH_3); 3.26–3.39 (m, 3H, 2 × H5′, H5′); 3.13–3.17 (m, 1H, H5′); 2.90–3.03 (m, 3H, 2 × H2′, H2′); 2.40–2.44 (m, 1H, H2′); 2.03–2.10 (m, 4H, CH_2CH_2OAr); 0.85 (s, 9H, $SiC(CH_3)_3$); 0.07 (s, 3H, $SiCH_3$); 0.00 (s, 3H, $SiCH_3$). MS (ESI): *m/z* calcd for $C_{88}H_{95}N_{10}O_{16}Si$ $[M+H]^+$, 1575.7 found 1575.7.

1-{O⁶-[3′-*O*-*tert*-butyldimethylsilyl-5′-*O*-dimethoxytrityl-N²-phenoxyacetyl-2′-deoxyguanidyl]}-7-{O⁶-[5′-*O*-dimethoxytrityl-N²-phenoxyacetyl-2′-deoxyguanidyl]}-heptane (6b)

To a solution of compound **5b** (0.52 g, 0.31 mmol) in anhydrous THF (3 mL) was added triphenylphosphine (24.4 mg, 0.09 mmol), palladium(0) tetrakistriphenylphosphine (35.2 mg, 0.03 mmol) and a butylamine/formic acid solution (1 : 1, 0.66 mmol) in THF (1 mL). After stirring at room temperature for 40 min the reaction was concentrated, taken up in CH_2Cl_2 (25 mL) and washed twice with 5% sodium bicarbonate (25 mL). The organic layer was then dried over sodium sulfate and evaporated. The crude was purified by silica gel column chromatography using a gradient of hexanes/ethyl acetate (1 : 0 → 1 : 4) to yield 0.376 g (76.0%) of a colorless foam. R_f (SiO_2): 0.33 hexanes/ethyl acetate (1 : 4). ^{1}H NMR (300 MHz, $CDCl_3$, ppm): 8.76 (s, 1H, NH); 8.67 (s, 1H, NH); 8.03 (s, 1H, H8); 8.01 (s, 1H, H8); 7.14–7.44 (m, 22H, Ar); 6.97–7.09 (m, 6H, Ar); 6.74–6.84 (m, 8H, Ar); 6.60 (dd, 1H, H1′, J = 6.6); 6.43 (dd, 1H, H1′, J = 6.4); 4.40–4.85 (m, 10H, 2 × H3′, 2 × $PhOCH_2CO$, 2 × CH_2OAr); 4.17–4.26 (m, 1H, H4′); 4.05–4.14 (m, 1H, H4′); 3.77 (s, 6H, OCH_3); 3.75 (s, 6H, OCH_3); 3.45 (dd, 1H, H5′); 3.00–3.38 (m, 3H, H5′, 2 x H5′); 3.21 (s, 1H, 3′OH); 2.56–2.83 (m, 3H, 2 × H2′, H2′); 2.40–2.51 (m, 1H, H2′); 1.90 (m, 4H, CH_2CH_2OAr); 1.52; (s, 6H, $(CH_2)_3$); 0.86 (s, 9H, $SiC(CH_3)_3$); 0.00 (s, 3H, $SiCH_3$); –0.05 (s, 3H, $SiCH_3$). MS (ESI): *m*/*z* calcd for $C_{91}H_{100}N_{10}O_{16}SiNa$ $[M+Na]^+$, 1639.7, found 1639.5.

1-{O⁶-[3′-*O*-*tert*-butyldimethylsilyl-5′-*O*-dimethoxytrityl-N²-phenoxyacetyl-2′-deoxyguanidyl]}-4-{O⁶-[5′-*O*-dimethoxytrityl-N²-phenoxyacetyl-2′-deoxyguanidyl-3′-*O*-(β-2-cyanoethyl-*N*,*N*′-diisopropyl)phosphoramidite]}-butane (7a)

Compound **6a** (0.45 g, 0.29 mmol) was dissolved in THF (1.4 mL) and diisopropylethylamine (0.055 g, 0.43 mmol) followed by *N*,*N*-diisopropylamino cyanoethyl phosphonamidic chloride (0.081 g, 0.343 mmol). The reaction was stirred at room temperature for 2 h after which it was quenched by the addition of ethyl acetate (50 mL) and the solution washed twice with 5% sodium bicarbonate (50 mL). The organic layer was dried over sodium sulfate, filtered and evaporated. The product was precipitated from vigorously stirring hexanes to give 0.43 g (86%) of a colorless powder. R_f (SiO_2): 0.64, 0.70 in ethyl acetate. ^{31}P NMR (121.5 MHz, acetone-d_6, ppm): 143.92, 144.14. MS (ESI): *m*/*z* calcd for $C_{97}H_{111}N_{12}O_{17}PSiNa$ $[M+Na]^+$, 1797.8, found 1797.6.

1-{O⁶-[3′-*O*-*tert*-butyldimethylsilyl-5′-*O*-dimethoxytrityl-N²-phenoxyacetyl-2′-deoxyguanidyl]}-7-{O⁶-[5′-*O*-dimethoxytrityl-N²-phenoxyacetyl-2′-deoxyguanidyl-3′-*O*-(β-2-cyanoethyl-*N*,*N*′-diisopropyl)phosphoramidite]}-heptane (7b)

Compound **6b** (0.35 g, 0.22 mmol) was dissolved in THF (1.1 mL) and diisopropylethylamine (0.042 g, 0.32 mmol) followed by *N*,*N*-diisopropylamino cyanoethyl phosphonamidic chloride (0.061 g, 0.26 mmol). The reaction stirred at room temperature for 2 h after which it was quenched by the addition of ethyl acetate (40 mL) and the solution washed twice with 5% sodium bicarbonate (50 mL). The organic layer was dried over sodium sulfate, filtered and evaporated. The product was precipitated from vigorously stirring hexanes to give 0.28 g (71%) of a colorless powder. R_f (SiO_2): 0.71, 0.82 in ethyl acetate. ^{31}P NMR (121.5 MHz, acetone-d_6, ppm): 143.91, 144.11. MS (ESI): *m*/*z* calcd for $C_{100}H_{117}N_{12}O_{17}PSiNa$ $[M+Na]^+$, 1839.8, found 1839.5.

Oligonucleotide synthesis, purification and characterization

The cross-linked duplexes **XL4** and **XL7**, whose sequences are shown in Fig. 1, were assembled using an Applied Biosystems Model 3400 synthesizer on a 1 μmole scale employing standard β-cyanoethylphosphoramidite cycles supplied by the manufacturer with slight modifications to coupling times described below. The nucleoside phosphoramidites containing standard protecting groups were prepared in anhydrous acetonitrile at a concentration of 0.1 M for the 3′-*O*-2′-deoxyphosphoramidites, 0.15 M for the cross-linked 3′-*O*-2′-deoxyphosphoramidites (**7a** and **7b**) and 0.2 M for the 5′-*O*-2′-deoxyphosphoramidites. Assembly of sequences first involved detritylation (3% trichloroacetic acid [TCA] in CH_2Cl_2), followed by nucleoside phosphoramidite coupling with commercial 3′-*O*-2′-deoxyphosphoramidites (2 min), 5′-*O*-2′-deoxyphosphoramidites (3 min) or cross-linked phosphoramidites **7a** or **7b** (10 min); subsequent capping with phenoxyacetic anhydride/pyridine/tetrahydrofuran (1 : 1 : 8, v/v/v; solution A, and 1-methyl-1 H-imidazole/tetrahydrofuran 16 : 84 w/v; solution B) and oxidation (0.02 M iodine in tetrahydrofuran–water/pyridine 2.5 : 2 : 1) followed every coupling. To complete assembly of the cross-linked duplexes, the cyanoethyl groups were removed from the polystyrene-linked oligomers by treating the support with 1 mL of anhydrous triethylamine (TEA) for at least 12 h. The support was then washed with 30 mL of anhydrous acetonitrile (ACN) followed by anhydrous THF. The *tert*-butyldimethylsilyl (TBS) group was removed from the partial duplex by treating the support with 2 × 1 mL triethylamine trihydrofluoride (TEA·3HF) for a total of 1 h. The support was then washed with 30 mL each of anhydrous THF and ACN followed by drying *via* high vacuum (20 min). The final extension of the cross-linked duplex was then achieved using 5′-*O*-2′-deoxyphosphoramidites with a total detritylation exposure of 130 s and removal of the 3′-terminal trityl group by the synthesizer to yield duplexes **XL4** and **XL7** on the solid support.

The oligomer-derivatized polystyrene beads were transferred from the reaction column to screw cap microfuge tubes fitted with teflon lined caps and the oligomer released from the support and protecting groups removed by treatment with a mixture of concentrated ammonium hydroxide/ethanol (0.3 mL : 0.1 mL) for 4 h at 55 °C. The cross-linked final products were separated from pre-terminated products by strong anion exchange (SAX) HPLC using a Dionex DNAPAC PA-100 column (0.4 cm x 25 cm) purchased from Dionex Corp, (Sunnyvale, CA) with a linear gradient of 0–50% buffer B over 30 min (buffer A: 100 mM Tris HCl, pH 7.5, 10% acetonitrile and buffer B: 100 mM Tris HCl, pH 7.5, 10% acetonitrile, 1 M NaCl) at 40 °C. The columns were monitored at 260 nm for analytical runs or 280 nm for preparative runs. The purified oligomers were desalted using C-18 SEP PAK cartridges (Waters Inc.) as previously described.[5] The amounts of purified oligomers obtained are shown in Table 1.

The cross-linked oligomers (0.1 A_{260} units) were characterized by enzymatic digestion (snake venom phosphodiesterase: 0.28 units and calf intestinal phosphatase: 5 units, in 10 mM Tris, pH 8.1 and 2 mM magnesium chloride) for a minimum of 36 h at 37 °C as previously described.[5] The resulting mixture

of nucleosides was analyzed by reversed phase HPLC carried out using a Symmetry® C-18 5 μm column (0.46 × 15 cm) purchased from Waters Inc, Milford, MA. The C-18 column was eluted with a linear gradient of 0–60% buffer B over 30 min (buffer A: 50 mM sodium phosphate, pH 5.8, 2% acetonitrile and buffer B: 50 mM sodium phosphate, pH 5.8, 50% acetonitrile). The resulting peaks were identified by co-injection with the corresponding standards and eluted at the following times: dC (4.6 min), dG (7.9 min), dT (8.5 min), dA (9.6 min), cross-link dimers (18.1 for the four carbon and 25.5 min for the seven carbon cross-link), and the ratio of nucleosides was determined. The results are given in Table 1. The molecular weights of the cross-linked oligomers were determined by ESI-MS and these were in agreement with the calculated values (see ESI for mass spectra†).

UV thermal denaturation studies

Molar extinction coefficients for the oligonucleotides and cross-linked duplexes were calculated from those of the mononucleotides and dinucleotides according to nearest-neighbour approximations (M^{-1} cm^{-1}). Non-cross-linked duplexes were prepared by mixing equimolar amounts of the interacting strands and lyophilizing the mixture to dryness. The resulting pellet was then re-dissolved in 90 mM sodium chloride, 10 mM sodium phosphate, 1 mM EDTA buffer (pH 7.0) to give a final concentration of 2.8 μM duplex. The cross-linked duplexes were dissolved in the same buffer to give a final concentration of 2.8 μM. The solutions were then heated to 90 °C for 10 min, cooled slowly to room temperature, and stored at 4 °C overnight before measurements. Prior to the thermal run, samples were degassed by placing them in a speed-vac concentrator for 2 min. Denaturation curves were acquired at 260 nm at a rate of heating of 0.5 °C min^{-1}, using a Varian CARY Model 3E spectrophotometer fitted with a 6-sample thermostated cell block and a temperature controller. The data were analyzed in accordance with the convention of Puglisi and Tinoco[50] and transferred to Microsoft Excel™.

Circular dichroism (CD) spectroscopy

Circular dichroism spectra were obtained on a Jasco J-815 spectropolarimeter equipped with a Julaba F25 circulating bath. Samples were allowed to equilibrate for 5–10 min at 10 °C in 90 mM sodium chloride, 10 mM sodium phosphate, 1 mM EDTA (pH 7.0), at a final concentration of 2.8 μM for the cross-linked duplexes and *ca.* 2.8 μM for control duplexes. Each spectrum was an average of 5 scans. Spectra were collected at a rate of 100 nm min^{-1}, with a bandwidth of 1 nm and sampling wavelength of 0.2 nm using fused quartz cells (Starna 29-Q-10). The CD spectra were recorded from 350 to 200 nm at 10 °C. The molar ellipticity was calculated from the equation $[\phi] = \varepsilon / Cl$, where ε is the relative ellipticity (mdeg), C is the molar concentration of oligonucleotides (moles/L), and l is the path length of the cell (cm). The data were processed on a PC computer using Windows™ based software supplied by the manufacturer (JASCO, Inc.) and transferred into Microsoft Excel™ for presentation.

Molecular modeling of ICL duplexes

The DNA duplex (5′-dCGATGTCATCG)/(5′-CGATGACATCG) and cross-linked duplexes **XL4** and **XL7** were built using HyperChem™ molecular modeling software. All duplexes were geometry optimized using the AMBER forcefield.

Protein expression and purification

Site directed mutagenesis as well as transformation into XL-10 *E. coli* cells were performed as directed by the Stratagene manual. Cells containing either a plasmid coding for wild-type or mutant hAGT were grown in a 1 L cultures of LB broth + 100 μg mL^{-1} ampicillin until an $OD_{600} = 0.6$ was reached. The cells were induced with 0.3 mM IPTG, incubated at 37 °C for 4 h with shaking at 225 rpm and harvested by centrifugation at 6000 × g at 4 °C for 30 min. Pellets were weighed and resuspended in 5 mL of buffer [20 mM Tris HCl (pH 8.0), 250 mM NaCl, 20 mM β-mercaptoethanol supplemented with Complete, Mini, EDTA-free Protease Inhibitor Cocktail Tablets] for each gram of pellet. The cells were homogenized by using approximately 20 strokes in a dounce homogenizer, lysed using two rounds of French press, centrifuged at 17000 × g for 45 min at 4 °C. The lysate was applied to a pre-equilibrated Ni-NTA Superflow column (100 mL resuspension buffer) containing 3.5 mL of resin. The lysate was run twice through the column at 1 mL min^{-1} to ensure complete binding. The column was washed with 200 mL resuspension buffer and 20 mM imidazole at 1 mL min^{-1}, until the OD_{280} of the eluant was constant. The protein eluted with 50 mL resuspension buffer supplemented with 200 mM imidazole at 1 mL min^{-1}. 1 mL fractions were collected and fractions that displayed protein content (generally fractions 4–11) were pooled followed by dialysis *versus* 4 L of dialysis buffer [50 mM Tris HCl (pH 7.6), 250 mM NaCl, 20 mM β-mercaptoethanol and 0.1 mM EDTA] using 8000 Da cutoff dialysis tubing. Typically a yield of 8–10 mg of purified protein was obtained per liter of culture inoculated.

Protein characterization

All proteins were analyzed by ESI-MS and were prepared by precipitation using one volume of TCA for every four volumes of protein. Samples were incubated for 10 min on ice, centrifuged at 4 °C for 5 min at 14 krpm on a table-top centrifuge, the supernatant removed, the pellet washed with 200 μL of cold acetone and washing repeated. The protein pellet was dried at 95 °C for 5 min, resuspended in a 50% acetonitrile and 1% formic acid solution at a protein concentration of 10 μM. The samples were analyzed with a Waters Micromass Q-ToF-2 mass spectrometer operating in positive-ion mode.

Far-UV circular dichroism (CD) spectra were obtained on a JASCO 815 spectropolarimeter using a 2 mm path length cell. The scans were performed at 20 °C, by averaging 5 wavelength scans from 260 to 200 nm (1 nm bandwidth) in 0.2 nm steps at a rate of 20 nm min^{-1}, and 1 s response at a protein concentration of 5 μM in CD buffer [50 mM potassium phosphate (pH 7.5), 75 mM NaCl and 2 mM dithiothreitol (DTT)].

Thermal denaturation curves were obtained by monitoring the change in mdeg at 222 nm (corresponding to the α-helical content of the protein). The heating rate was set at 15 °C h^{-1} using a Peltier-type temperature controller, which ranged from 40–70 °C. The T_m was obtained by noting the temperature at which the 1st derivative of the denaturation plot was the highest.

Fluorescence spectra were obtained using a Varian Cary Eclipse Fluorescence Spectrophotometer in a 10 mm quartz cuvette with 3.5 μM protein in CD buffer at room temperature. Excitation and emission slits were set at 5 nm with a detector voltage of 650 and the spectra were the average of 10 accumulations. Tyrosine and tryptophan fluorescence were obtained using an excitation wavelength of 280 nm and recording the emission spectrum between 300 and 400 nm. To monitor the tryptophan fluorescence solely an excitation wavelength of 295 nm was used and the emission spectrum was monitored between 300 and 400 nm.

Denaturing polyacrylamide gel electrophoresis assay of O^6-dG-alkyl-O^6-dG interstrand cross-link repair

The cross-linked oligonucleotides **XL4** and **XL7** as well as the control DNA (non-cross-linked duplex) were labeled at the 5′-end using [γ-^{32}P]ATP. 10 μL reaction volumes were used for the labeling of the DNA. The reaction mixture was comprised of 1 × T4 PNK buffer (Fermentas), 21 μM oligonucleotides, 10 μM cold-ATP, 1 μL [γ-^{32}P]ATP (10 μCi/μL) and 5 units of T4 PNK. The reaction mixture was incubated at 37 °C for 1 h and terminated by placing the reaction in boiling water for 10 min. 60 pmol of wild-type and mutant hAGT protein was incubated with 2 pmol of labeled DNA in a total reaction volume of 15 μL comprised of hAGT buffer [80 mM Tris HCl (pH 7.6), 0.1 mM EDTA and 5 mM DTT]. The reactions were incubated at 37 °C for 14 to 16 h with similar results indicating that the reaction was complete by 14 h. Denaturing PAGE in 7 M urea was used to analyze the products. The reaction was terminated by adding 18.2 μL of stop reaction buffer [81 mM Tris-HCl, 81 mM boric acid, 1.8 mM EDTA and 1% SDS (pH 8.0) in 80% formamide] to the reaction tube and heating as above. The samples were loaded onto 14 cm × 16 cm, 17% polyacrylamide gels (19 : 1) in the presence of 7 M urea. The gels were run using 1 × TBE [89 mM Tris-HCl, 89 mM boric acid, 2 mM EDTA (pH 8.0)] for 1.5 h at 700 V, which heated the gels to 40 °C. After electrophoresis, the gels were covered in Saran wrap and exposed to a storage phosphor screen. The image was captured using a Typhoon 9400 (GE Healthcare, Piscataway, NJ) and the counts of the radiolabelled products quantified using ImageQuant™ (Amersham Biosciences). A control lane was used as a standard in order to quantitate the other bands on the gel. For the repair time course assay of the ICLs a 150 μL master mix composed of 600 pmol of wild-type hAGT and 20 pmol of DNA substrate in hAGT buffer was prepared. The sample was placed at 37 °C. At every time point 7.5 μL (1 pmol of DNA) was removed from the master mix and placed in a tube with 9.1 μL of stop reaction buffer and terminated as above.

Binding studies of C145S hAGT using protein titration

Reaction tubes consisting of 5 nM DNA and increasing C145S hAGT concentrations (ranging from 1 to 35.69 μM) were prepared in a total solution volume of 20 μl of binding buffer [10 mM Tris-HCl (pH 7.6), 5 mM DTT and 0.1 mM EDTA]. The samples were allowed to equilibrate on ice for 30 min. Triplicate samples were incubated for longer (45 min and 2 h) and yielded similar results indicating that equilibrium had been attained. Each sample (0.1 pmol) was loaded on 14 cm x 16 cm, 4 °C, preequilibrated native 6% polyacrylamide (75 : 1) gels. The gels were electrophoresed in 10 mM Tris acetate (pH 7.6) and 0.25 mM EDTA buffer at 125 V for 1 h. On completion, the gels were covered and processed as described above.

Estimates of the monomeric dissociation constant (K_d) and the cooperativity factor (n) were obtained from the electrophoretic mobility shift assays as explained previously.[48] The binding of n moles of hAGT protein [P] to 1 mole of cross-linked DNA [D] follows the equation: $nP + D \leftrightarrow P_nD$. Isolating the variables and taking the logarithm of the equation yields:

$$\log\left(\frac{[P_nD]}{[D]}\right) = n \log [P]_{free} + \log K_d$$

Plotting log $[P_nD]/[P]$ as a function of log [P] gives a slope equal to n. At half-saturation: log $[P_nD]/[P] = 0$ and observed K_d can be obtained from the relation observed $K_d = -n \ln [P]$. The monomeric K_d can be obtained by taking the nth root of the observed K_d.

Colony forming assay in CHO cells treated with busulfan and hepsulfam

CHO cells transfected with either the empty pCMV vector or pCMV-hAGT were grown in α-MEM media (Gibco-Invitrogen, Carlsbad, CA) containing 26 mM $NaHCO_3$, 10% fetal bovine serum (Atlanta Biologicals, Lawrenceville, CA), 100 U/ml penicillin and 100 μg ml^{-1} streptomycin. The cells were maintained by seeding at 1×10^5 cells/25 cm^2 flask at weekly intervals. For colony forming assays, cells were plated at a density of 10^6 per 25 cm^2 flask and 24 h later were treated with different concentrations of busulfan (Sigma, St Louis, MO) or hepsulfam (NCI, Frederick, MD) for 4 h. The cells were washed with phosphate buffered saline (PBS) twice, and then the medium was replaced with fresh medium and the cells allowed to grow for another 16–18 h. They were then replated at densities of 250–1000 cells per 25 cm^2 flask and grown for 6–8 days until discrete colonies had formed. The colonies were washed with 0.9% saline solution, stained with 0.5% crystal violet and counted.

Acknowledgements

We thank the Natural Sciences and Engineering Research Council of Canada (NSERC), the Canada Foundation for Innovation (CFI), the Canada Research Chair (CRC) program (to CJW) and grant CA-018137 from the NCI, US Public Health Service (to AEP) for financial support of this project. FPM is the recipient of graduate fellowships from NSERC, the Fonds Québécois de la Recherche sur la Nature et les Technologies (FQRNT) and Groupe de Recherche Axé sur la Structure des Protéines (GRASP). We also thank Mr Nadim Saadeh and Dr Bruce Lennox of McGill University for ESI-MS analysis.

References

1 M. L. Dronkert and R. Kanaar, *Mutat. Res.*, 2001, **486**, 217.
2 S. R. Rajski and R. M. Williams, *Chem. Rev.*, 1998, **98**, 2723.
3 D. M. Noll, T. M. Mason and P. S. Miller, *Chem. Rev.*, 2006, **106**, 277.
4 J. Alzeer and O. D. Schärer, *Nucleic Acids Res.*, 2006, **34**, 4458.
5 C. J. Wilds, F. Xu and A. M. Noronha, *Chem. Res. Toxicol.*, 2008, **21**, 686.
6 T. Angelov, A. Guainazzi and O. D. Schärer, *Org. Lett.*, 2009, **11**, 661.
7 K. Stevens and A. Madder, *Nucleic Acids Res.*, 2009, **37**, 1555.

8 M. M. Ali, S. Imoto, Y. Li, S. Sasaki and F. Nagatsugi, *Bioorg. Med. Chem.*, 2009, **17**, 2859.
9 Y. Taniguchi, Y. Kurose, T. Nishioka, F. Nagatsugi and S. Sasaki, *Bioorg. Med. Chem.*, 2010, **18**, 2894.
10 H. Huang, H. Y. Kim, I. D. Kozekov, Y. J. Cho, H. Wang, A. Kozekova, T. M. Harris, C. J. Rizzo and M. P. Stone, *J. Am. Chem. Soc.*, 2009, **131**, 8416.
11 D. M. Noll, M. Webba da Silva, A. M. Noronha, C. J. Wilds, O. M. Colvin, M. P. Gamcsik and P. S. Miller, *Biochemistry*, 2005, **44**, 6764.
12 P. M. Ravdin, K. A. Havlin, M. V. Marshall, T. D. Brown, J. M. Koeller, J. G. Kuhn, G. Rodriguez and D. D. Von Hoff, *Cancer Res.*, 1991, **51**, 6268.
13 R. T. Streeper, R. J. Cotter, M. E. Colvin, J. Hilton and O. M. Colvin, *Cancer Res.*, 1995, **55**, 1491.
14 J. A. Haines, C. B. Reese and T. Lord, *J. Chem. Soc.*, 1962, 5281.
15 R. K. Robins and L. B. Townsend, *J. Am. Chem. Soc.*, 1963, **85**, 252.
16 C. J. Wilds, J. D. Booth and A. M. Noronha, *Tetrahedron Lett.*, 2006, **47**, 9125.
17 O. Khan and M. R. Middleton, *Expert Opin. Invest. Drugs*, 2007, **16**, 1573.
18 F. Himmelsbach, B. S. Schulz, T. Trichtinger, R. Charubala and W. Pfleiderer, *Tetrahedron*, 1984, **40**, 59.
19 T. Shibata, N. Glynn, T. B. H. McMurry, R. S. McElhinney, G. P. Margison and D. M. Williams, *Nucleic Acids Res.*, 2006, **34**, 1884.
20 O. Mitsunobu, *Synthesis*, 1981, 1.
21 A. E. Pegg, *Mutat. Res.*, 2000, **462**, 83.
22 D. S. Daniels, T. T. Woo, K. X. Luu, D. M. Noll, N. D. Clarke, A. E. Pegg and J. A. Tainer, *Nat. Struct. Mol. Biol.*, 2004, **11**, 714.
23 K. S. Srivenugopal, X. H. Yuan, H. S. Friedman and F. Ali-Osman, *Biochemistry*, 1996, **35**, 1328.
24 R. Coulter, M. Blandino, J. M. Tomlinson, G. T. Pauly, M. Krajewska, R. C. Moschel, L. A. Peterson, A. E. Pegg and T. E. Spratt, *Chem. Res. Toxicol.*, 2007, **20**, 1966.
25 I. Buggia, F. Locatelli, M. B. Regazzi and M. Zecca, *Ann. Pharmacother.*, 1994, **28**, 1055.
26 W. P. Tong and D. B. Ludlum, *Biochim. Biophys. Acta, Nucleic Acids Protein Synth.*, 1980, **608**, 174.
27 T. Iwamoto, Y. Hiraku, S. Oikawa, H. Mizutani, M. Kojima and S. Kawanishi, *Cancer Sci.*, 2004, **95**, 454.
28 Y. Hayakawa, H. Kato, M. Uchiyama, H. Kajino and R. Noyori, *J. Org. Chem.*, 1986, **51**, 2400.
29 R. S. Braich and M. J. Damha, *Bioconjugate Chem.*, 1997, **8**, 370.
30 Q. Zhu, M. O. Delaney and M. M. Greenberg, *Bioorg. Med. Chem. Lett.*, 2001, **11**, 1105.
31 M. J. Damha and K. K. Ogilvie, in *Methods in Molecular Biology*, ed. S. Agrawal, The Humana Press, Inc. Totowa, NJ, 1993, vol. 20, pp. 81–114.
32 B. L. Gaffney, L. A. Marky and R. A. Jones, *Biochemistry*, 1984, **23**, 5686.
33 B. L. Gaffney and R. A. Jones, *Biochemistry*, 1989, **28**, 5881.
34 S. Kuzmich, L. A. Marky and R. A. Jones, *Nucleic Acids Res.*, 1983, **11**, 3393.
35 W. C. Johnson Jr., in *Methods of Biochemical Analysis*, ed. D. Glick, Wiley, New York, 1985, vol. 31, pp. 61.
36 W. C. Johnson Jr., in *Circular Dichroism and the Conformational Analysis of Biomolecules*, ed.G. D. Fasman, Plenum Press, New York, 1996, pp. 433.
37 D. J. Patel, L. Shapiro, S. A. Kozlowski, B. L. Gaffney and R. A. Jones, *Biochemistry*, 1986, **25**, 1027.
38 J. J. Rasimas, A. E. Pegg and M. G. Fried, *J. Biol. Chem.*, 2003, **278**, 7973.
39 T. M. Crone and A. E. Pegg, *Cancer Res.*, 1993, **53**, 4750.
40 T. M. Crone, K. Goodtzova, S. Edara and A. E. Pegg, *Cancer Res.*, 1994, **54**, 6221.
41 D. S. Daniels, C. D. Mol, A. S. Arvai, S. Kanugula, A. E. Pegg and J. A. Tainer, *EMBO J.*, 2000, **19**, 1719.
42 S. Kanugula and A. E. Pegg, *Biochem. J.*, 2003, **375**, 449.
43 K. Goodtzova, T. M. Crone and A. E. Pegg, *Biochemistry*, 1994, **33**, 8385.
44 Q. Fang, A. M. Noronha, S. P. Murphy, C. J. Wilds, J. L. Tubbs, J. A. Tainer, G. Chowdhury, F. P. Guengerich and A. E. Pegg, *Biochemistry*, 2008, **47**, 10892.
45 J. J. Rasimas, A. E. Pegg and M. G. Fried, *J. Biol. Chem.*, 2003, **278**, 7973.
46 J. J. Rasimas, P. A. Dalessio, I. J. Ropson, A. E. Pegg and M. G. Fried, *Protein Sci.*, 2004, **13**, 301.
47 R. Coulter, M. Blandino, J. M. Tomlinson, G. T. Pauly, M. Krajewska, R. C. Moschel, L. A. Peterson, A. E. Pegg and T. E. Spratt, *Chem. Res. Toxicol.*, 2007, **20**, 1966.
48 M. G. Fried, S. Kanugula, J. L. Bromberg and A. E. Pegg, *Biochemistry*, 1996, **35**, 15295.
49 E. M. Duguid, P. A. Rice and C. He, *J. Mol. Biol.*, 2005, **350**, 657.
50 J. D. Puglisi and I. J. Tinoco, *Methods Enzymol.*, 1989, **180**, 304.

